THE UNIVERSITY OF
WARWICK

University of Warwick institutional repository: http://go.warwick.ac.uk/wrap

This paper is made available online in accordance with publisher policies. Please scroll down to view the document itself. Please refer to the repository record for this item and our policy information available from the repository home page for further information.

To see the final version of this paper please visit the publisher's website. Access to the published version may require a subscription.

Search for Lepton Number Violating Decays $B^+ \to \pi^- \mu^+ \mu^+$ and $B^+ \to K^- \mu^+ \mu^+$

R. Aaij *et al.**
(LHCb Collaboration)

A search is performed for the lepton number violating decay $B^+ \to h^- \mu^+ \mu^+$, where h^- represents a K^- or a π^-, using an integrated luminosity of 36 pb^{-1} of data collected with the LHCb detector. The decay is forbidden in the standard model but allowed in models with a Majorana neutrino. No signal is observed in either channel and limits of $\mathcal{B}(B^+ \to K^- \mu^+ \mu^+) < 5.4 \times 10^{-8}$ and $\mathcal{B}(B^+ \to \pi^- \mu^+ \mu^+) < 5.8 \times 10^{-8}$ are set at the 95% confidence level. These improve the previous best limits by factors of 40 and 30, respectively.

Gauge invariance of the electromagnetic field results in electric charge conservation but there is no known symmetry associated with lepton number conservation. The apparent conservation of lepton number in the standard model is therefore one of the fundamental puzzles in particle physics. New physics models such as those with Majorana neutrinos [1] or left-right symmetric models with a doubly charged Higgs boson [2] can violate lepton number conservation and searches for lepton number violating decays are therefore of fundamental importance. Such decays have previously been searched for in both rare decay processes [3–5] and in same-sign dilepton searches [6].

In this Letter a search for lepton number violating decays of the type $B^+ \to h^- \mu^+ \mu^+$, where h^- represents a K^- or a π^-, is presented. The inclusion of charge conjugate modes is implied throughout. A search for any lepton number violating process that mediates the $B^+ \to h^- \mu^+ \mu^+$ decay is made. A specific search for $B^+ \to h^- \mu^+ \mu^+$ decays mediated by an on-shell Majorana neutrino is also performed (Fig. 1). Such decays would give rise to a narrow peak in the invariant mass spectrum of the hadron and one of the muons [7], $m_\nu = m_{h\mu}$, if the mass of the neutrino is between $m_{K(\pi)} + m_\mu$ and $m_B - m_\mu$. Theoretical predictions for the $B^+ \to h^- \mu^+ \mu^+$ branching fractions in Majorana neutrino models depend on the Majorana neutrino's mass and its mixing parameter with light neutrinos. As an example, in the $B^+ \to K^- \mu^+ \mu^+$ decay mode, theoretical models predict branching fractions could be at the 10^{-6} level given present experimental constraints [8]. This branching fraction is just below the previous best limits for $B^+ \to K^-(\pi^-)\mu^+\mu^+$

decays which are $<1.8(1.2) \times 10^{-6}$ at 90% confidence level (C.L.) [4].

Constraints on doubly charged Higgs models have been derived from indirect searches with an off-shell H^{++} [9]. For example, searches for the decay $\tau^+ \to \mu^+ \mu^+ \mu^-$ set limits in the coupling versus H^{++} mass plane. Whereas this process requires both lepton flavor and lepton number violating couplings, $B^+ \to h^- \mu^+ \mu^+$ decays do not involve any lepton flavor violation. The coupling in such decays might therefore be larger. We are not aware of any theoretical papers which derive limits on these couplings from existing experimental limits on $B^+ \to h^- \mu^+ \mu^+$ branching fractions. For $K^+ \to \pi^- \mu^+ \mu^+$ decays the potential contribution from H^{++} is of comparable size to that from Majorana neutrinos [10].

The search for $B^+ \to h^- \mu^+ \mu^+$ is carried out with data from the LHCb experiment [11] at the Large Hadron Collider. The data correspond to 36 pb^{-1} of integrated luminosity of proton-proton collisions at $\sqrt{s} = 7$ TeV collected in 2010. The LHCb detector is a single-arm spectrometer designed to study b-hadron decays with an acceptance for charged tracks with pseudorapidity between 2 and 5. Primary proton-proton vertices (PVs), and secondary B vertices are identified in a silicon strip vertex detector. Tracks from charged particles are reconstructed by the vertex detector and a set of tracking stations. The curvature of the tracks in a dipole magnetic field allows momenta to be determined with a precision of $\delta p/p = 0.4\%–0.6\%$. Two ring imaging Cherenkov (RICH) detectors allow
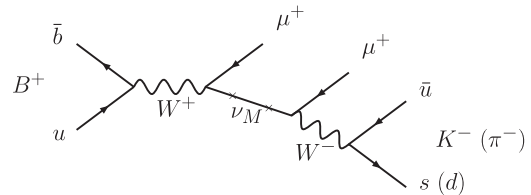
FIG. 1. s-channel diagram for $B^+ \to K^- \mu^+ \mu^+$ ($B^+ \to \pi^- \mu^+ \mu^+$) where the decay is mediated by an on-shell Majorana neutrino.

101601-1

kaons to be separated from pions and muons over a momentum range $2 < p < 100$ GeV/c. Muons with momentum above 3 GeV/c are identified on the basis of the number of hits in detectors interleaved with an iron muon filter.

The search for $B^+ \rightarrow h^- \mu^+ \mu^+$ decays is based on the selection of $B^+ \rightarrow h^\pm \mu^+ \mu^\mp$ candidates. The $B^+ \rightarrow J/\psi K^+$ decay with $J/\psi \rightarrow \mu^+ \mu^-$ is included in the same selection. It is subsequently used as a normalization mode when setting a limit on the branching fraction of the $B^+ \rightarrow h^- \mu^+ \mu^+$ decays. The selection is designed to minimize and control the difference between decays with same- and opposite-sign muons and thus cancel most of the systematic uncertainty from the normalization. The only differences in efficiency between the signal and normalization channels are due to the decay kinematics and the presence of a same-sign muon pair, rather than an opposite-sign pair, in the final state.

In the trigger, the $B^+ \rightarrow h^\pm \mu^+ \mu^\mp$ candidates are required to pass the initial hardware trigger based on the p_T of one of the muons. In the subsequent software trigger, one of the muons is required to have a large impact parameter (IP) with respect to all the PVs in the event and to pass requirements on the quality of the track fit and the compatibility of the candidate with the muon hypothesis. Finally, the muon candidate combined with another track is required to form a vertex displaced from the PVs.

Further event selection is applied offline on fully reconstructed B decay candidates. The selection is designed to reduce combinatorial backgrounds, where not all the selected tracks come from the same decay vertex, and peaking backgrounds, where a single decay is selected but with some of the particle types misidentified. The combinatorial background is smoothly distributed in the reconstructed B-candidate mass and the level of background is assessed from the sidebands around the signal window. Peaking backgrounds from B decays to hadronic final states, final states with a J/ψ, and semileptonic final states are also considered.

Proxies are used in the optimization of the selection for both the signal and the background to avoid a selection bias. The $B^+ \rightarrow J/\psi K^+$ decay is used as a proxy for the signal. The background proxy comprises opposite-sign $B^+ \rightarrow h^+ \mu^+ \mu^-$ candidates with an invariant mass in the upper mass sideband and with muon pairs incompatible with a J/ψ or a $\psi(2S)$ hypothesis.

The combinatorial background is reduced by requiring that the decay products of the B have $p_T > 800$ MeV/c. Tracks are selected which are incompatible with originating from any PV in the event based on the χ^2 of the tracks' impact parameters ($\chi^2_{\text{IP}} > 45$). The direction of the candidate B^+ momentum is required to be within 8 mrad of the reconstructed B^+ line of flight. There are on average 2.5 PVs in an event and the PV used to compute the line of flight is that with respect to which the B^+ candidate has the smallest IP. The B^+ vertex is also required to be of good quality ($\chi^2 < 12$ for 3 degrees of freedom) and significantly displaced from the PV (χ^2 of vertex separation larger than 144 for 1 degree of freedom).

The selection uses a range of particle identification (PID) criteria, based on information from the RICH and muon detectors, to ensure the hadron and the muons are correctly identified. For example, $\text{DLL}_{K\pi}$ is the difference in log-likelihoods between the K and π hypotheses. For the $B^+ \rightarrow K^- \mu^+ \mu^+$ final state, $\text{DLL}_{K\pi} > 1$ is required to select kaon candidates. For the kinematic range considered, typical kaon identification efficiencies are around 90% with misidentification of pions as kaons at the few percent level. For the $B^+ \rightarrow \pi^- \mu^+ \mu^+$ final state the selection criterion is mirrored to select pions with $\text{DLL}_{K\pi} < -1$. The $B^+ \rightarrow K^- \mu^+ \mu^+$ and $B^+ \rightarrow \pi^- \mu^+ \mu^+$ selections are otherwise identical. In order to avoid selecting a muon as the pion or kaon, the candidate hadron is also required to be within the acceptance of the muon system but not have a track segment there. After the application of these criteria the combinatorial background is completely dominated by candidates with two real muons, rather than by hadrons misidentified as muons.

The invariant mass distribution and the relevant misidentification rates are required in order to evaluate the peaking background. These are evaluated, respectively, from a full simulation using PYTHIA [12] followed by GEANT4 [13], and from control channels which provide an unambiguous and pure source of particles of known type. The control channel events are selected to have the same kinematics as the signal decay, without the application of any PID criteria. $D^{*+} \rightarrow D^0 \pi^+$, $D^0 \rightarrow K^- \pi^+$ decays give pure sources of pions and kaons. A pure source of muons is isolated using a $J/\psi \rightarrow \mu^+ \mu^-$ sample where the muon identification requirement is applied to only one of the muons [14].

Under the $B^+ \rightarrow K^- \mu^+ \mu^+$ hypothesis, any crossfeed from $B^+ \rightarrow J/\psi K^+$ decays would peak strongly in the signal mass region. The $K \rightarrow \mu$ mis-ID rate is evaluated from the above D^* sample and the $\mu \rightarrow K$ mis-ID rate from the J/ψ sample. The later mis-ID rate is consistent with zero but with a large uncertainty. The number of $B^+ \rightarrow J/\psi K^+$ events expected in the signal region is therefore $(0.0^{+14.0}_{-0.0}) \times 10^{-3}$. The uncertainty on this background dominates the error on the total exclusive background expected in the signal region. The $B^+ \rightarrow \pi^- \pi^+ K^+$ decay contributes the most to the peaking background with an expected $(1.7 \pm 0.1) \times 10^{-3}$ candidates, followed by the $B^+ \rightarrow K^- \pi^+ K^+$ decay with $(6.1 \pm 0.8) \times 10^{-4}$ candidates. The total peaking background expected in the $B^+ \rightarrow K^- \mu^+ \mu^+$ signal region is $(3.4^{+14.0}_{-0.2}) \times 10^{-3}$ events with the asymmetric error caused by the zero expectation from the $B^+ \rightarrow J/\psi K^+$ decay.

Under the $B^+ \rightarrow \pi^- \mu^+ \mu^+$ hypothesis, $B^+ \rightarrow J/\psi K^+$ decays are reconstructed with invariant masses below the

nominal B^+ mass, in the lower mass sideband (masses in the range 5050–5240 MeV/c^2). The dominant background decay in this case is $B^+ \to \pi^- \pi^+ \pi^+$, where the two same-sign pions are misidentified as muons. The $B^+ \to \pi^- \mu^+ \mu^+$ peaking background level is $(2.9 \pm 0.6) \times 10^{-2}$ events.

In Fig. 2(a), the $m_{K^+ \mu^+ \mu^-}$ invariant mass distribution for $B^+ \to K^+ \mu^+ \mu^-$ events with $|m_{\mu^+ \mu^-} - m_{J/\psi}| <$ 50 MeV/c^2 is shown, after the application of the selection. In the $B^+ \to J/\psi K^+$ sample, there are no events containing more than one candidate. An unbinned maximum likelihood fit to the $B^+ \to J/\psi K^+$ mass peak is made with a crystal ball [15] function which accounts for the radiative tail. The combinatorial background is assumed to be flat, and the partially reconstructed events in the lower mass sideband are fitted with a Gaussian distribution. The $B^+ \to J/\psi K^+$ peak has a Gaussian component of width 20 MeV/c^2, and a mass window of 5280 ± 40 MeV/c^2 is chosen. The peak contains 3407 ± 59 $B^+ \to J/\psi K^+$ events within this window. $B^+ \to J/\psi \pi^+$ candidates were also examined and, accounting for a shoulder in the mass distribution from $B^+ \to J/\psi K^+$, the yield observed agrees with the expectation when using the branching fraction from Ref. [16].

The $m_{K^+ \mu^+ \mu^-}$ invariant mass distribution for events with $|m_{\mu^+ \mu^-} - m_{J/\psi}| > 70$ MeV/c^2 and $|m_{\mu^+ \mu^-} - m_{\psi(2S)}| > 70$ MeV/c^2 is shown in Fig. 2(b). Using the same fit model, with all shape parameters fixed to those from the above fit, the peak was determined to contain 27 ± 5 events from the $B^+ \to K^+ \mu^+ \mu^-$ decay. The ratio of branching fractions between $B^+ \to J/\psi K^+$ and $B^+ \to K^+ \mu^+ \mu^-$ decays [16] and the trigger efficiency ratio predicted by the simulation, give an expectation of 29 ± 4 $B^+ \to K^+ \mu^+ \mu^-$ decays. The observed yield is consistent with the expectation showing that the selection does not favor candidates with a dimuon mass close to the J/ψ mass.

The difference in efficiency between the signal and normalization channels was evaluated using Monte Carlo simulation samples. The relative selection efficiency across the phase space is shown for $B^+ \to K^- \mu^+ \mu^+$ in Fig. 3. The efficiency of the signal selection in a given phase-space bin is divided by the average efficiency of $B^+ \to J/\psi K^+$, to yield the relative efficiency for that bin. The D^* control channel is used to determine the PID efficiencies required to normalize $B^+ \to \pi^- \mu^+ \mu^+$ to $B^+ \to J/\psi K^+$.

Assuming a signal that is uniformly distributed in phase space, the relative efficiency of $B^+ \to K^- \mu^+ \mu^+$ and $B^+ \to J/\psi K^+$ was calculated to be $89.1 \pm 0.4(\text{stat}) \pm 0.3(\text{syst})\%$. The relative efficiency of $B^+ \to \pi^- \mu^+ \mu^+$ and $B^+ \to J/\psi K^+$ was calculated to be $82.7 \pm 0.6(\text{stat}) \pm 0.8(\text{syst})\%$. The systematic uncertainties associated with these estimates are detailed below. These relative efficiencies together with the number of events observed in the normalization channel and the $B^+ \to J/\psi K^+$ branching fraction taken from Ref. [16], give single event sensitivities of 2.0×10^{-8} (2.1×10^{-8}) in the $B^+ \to K^- \mu^+ \mu^+$ $(B^+ \to \pi^- \mu^+ \mu^+)$ case.

In order to compute the efficiency under a given Majorana neutrino mass hypothesis, a model for the
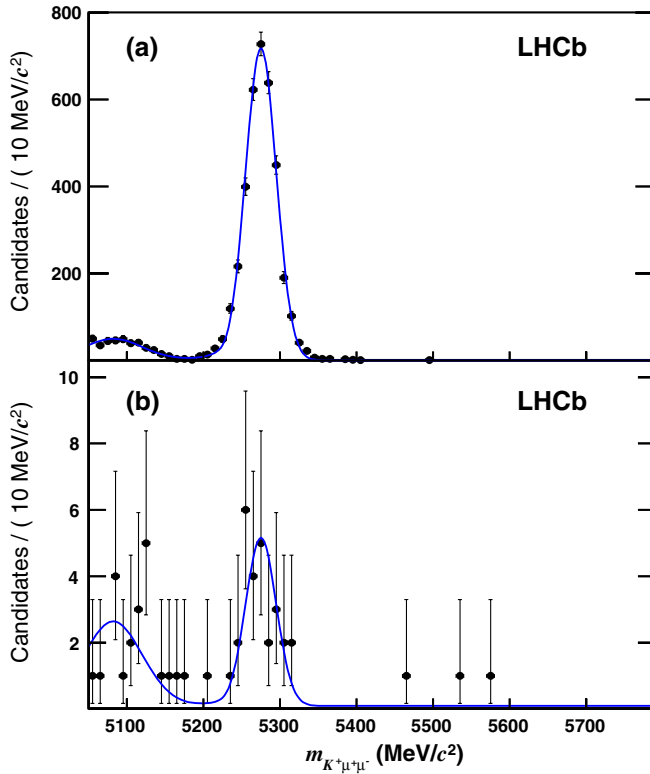

FIG. 2 (color online).   Invariant mass distribution of $K^+ \mu^+ \mu^-$ events after the application of the selection criteria. In (a) requiring the muon pair to be compatible with coming from a J/ψ decay and in (b) excluding invariant mass windows around the J/ψ and $\psi(2S)$ for the muon pair. The curve is the fit to data as described in the text.
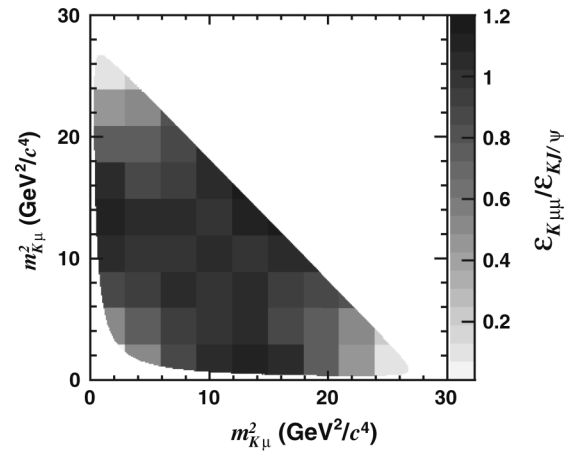

FIG. 3.   Relative efficiency between the $B^+ \to K^- \mu^+ \mu^+$ signal and the $B^+ \to J/\psi K^+$ normalization channel. The plot has been symmetrized over the diagonal.

variation of efficiency with $m_{h\mu}$ is required. For a given value of $m_{h\mu}$ this is obtained by varying the polarization of the Majorana neutrino in the decay and taking the lowest (most conservative) value of the efficiency.

The dominant systematic uncertainty (under the assumption of a flat phase-space distribution) for the single event sensitivity is the 3.4% uncertainty on the $B^+ \to J/\psi K^+$ branching fraction. The statistical uncertainty on the $B^+ \to J/\psi K^+$ yield gives an additional systematic uncertainty of 1.7% and the uncertainty from the model used to fit the data is 1.6%. The latter is evaluated by changing the crystal ball signal function used in the fit to a Gaussian and the polynomial background function to an exponential.

There are several sources of uncertainty associated with the calculation of the relative efficiency between the signal and normalization channels. In addition to the statistical uncertainty of the simulation samples, there are systematic uncertainties from the differences in the effect of the IP selection criteria between the simulation and data, the statistical uncertainty on the measured PID efficiencies, the uncertainties associated with the simulation of the trigger, and the uncertainty in the tracking efficiency. In each case the systematic uncertainty is estimated by varying the relevant criteria at the level of the expected effect and reevaluating the relative efficiency. For the $B^+ \to \pi^- \mu^+ \mu^+$ decay, there is an additional uncertainty from the correction for the relative kaon- and pion-identification efficiencies. The systematic uncertainties averaged over the three-body phase space are given in Table I.

A limit on the branching fraction of each of the $B^+ \to h^- \mu^+ \mu^+$ decays is set by counting the number of observed events in the mass windows, and using the single event sensitivity. The probability is modeled with a Poisson distribution where the mean has contributions from a potential signal, the combinatorial and peaking backgrounds. The combinatorial background is unconstrained by measurements from the simulation or the opposite-sign data. The number of events in the upper mass sideband is therefore used to constrain the contribution of the combinatorial background to the Poisson mean. The upper mass sideband is restricted to masses above $m_{h\mu\mu} > 5.4$ GeV/c^2 such

that any peaking background component can be ignored. In both the $B^+ \to K^- \mu^+ \mu^+$ and $B^+ \to \pi^- \mu^+ \mu^+$ cases no events are found in either the upper or lower mass sidebands. This is consistent with the observation of three opposite-sign candidates seen in the $B^+ \to K^+ \mu^+ \mu^-$ upper mass sideband (Fig. 2) and two candidates in the $B^+ \to \pi^+ \mu^+ \mu^-$ upper mass sideband. The peaking background estimates are explicitly split into two components, the contribution from $B^+ \to h^- h^+ h^+$ decays and that from $B^+ \to J/\psi K^+$ decays. The latter has a large uncertainty. The central values for both peaking background components are taken from the estimates described above.

Systematic uncertainties on the peaking background, single event sensitivity, and signal-to-sideband scale factor are included in the limit-setting procedure using a Bayesian approach. The unknown parameter is integrated over and included in the probability to observe a given number of events in the signal and upper mass window.

In the signal mass windows of $B^+ \to K^- \mu^+ \mu^+$ and $B^+ \to \pi^- \mu^+ \mu^+$ no events are observed. This corresponds to limits on the $B^+ \to h^- \mu^+ \mu^+$ branching fractions of

$$\mathcal{B}(B^+ \to K^- \mu^+ \mu^+) < 5.4(4.1) \times 10^{-8} \text{ at } 95\%(90\%) \text{ C.L.},$$

$$\mathcal{B}(B^+ \to \pi^- \mu^+ \mu^+) < 5.8(4.4) \times 10^{-8} \text{ at } 95\%(90\%) \text{ C.L.}$$

The observation of no candidates in the sidebands as well as the signal region is compatible with a background-only hypothesis. The $m_{h\mu}$ dependence of the limit in models where the Majorana neutrino can be produced on mass shell is shown in Fig. 4. The shapes of the limits arise from the changing efficiency as a function of mass.

In summary, a search for the $B^+ \to K^- \mu^+ \mu^+$ and $B^+ \to \pi^- \mu^+ \mu^+$ decay modes has been performed with 36 pb^{-1} of integrated luminosity collected with the LHCb detector in 2010. No signal is observed in either decay and, using $B^+ \to J/\psi K^+$ as a normalization channel, the

TABLE I. Sources of systematic error and their fractional uncertainty on the relative efficiency.

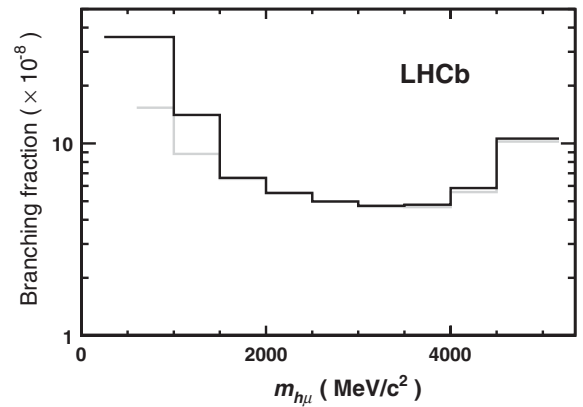| Source	$B^+ \to K^- \mu^+ \mu^+$	$B^+ \to \pi^- \mu^+ \mu^+$
$\mathcal{B}(B^+ \to J/\psi K^+)$	3.4%	3.4%
$B^+ \to J/\psi K^+$ yield	1.7%	1.7%
$B^+ \to J/\psi K^+$ fit models	1.6%	1.6%
Simulation statistics	0.4%	0.6%
IP modeling	0.2%	0.2%
PID modeling	0.1%	0.8%
Trigger efficiency	0.1%	0.1%
Tracking efficiency	0.1%	0.1%

FIG. 4. The 95% C.L. branching fraction limits for $B^+ \to K^- \mu^+ \mu^+$ (light-colored line) and $B^+ \to \pi^- \mu^+ \mu^+$ (dark-colored line) as a function of the Majorana neutrino mass $m_\nu = m_{h\mu}$.

present best limits on $\mathcal{B}(B^+ \to K^- \mu^+ \mu^+)$ and $\mathcal{B}(B^+ \to \pi^- \mu^+ \mu^+)$ are improved by factors of 40 and 30, respectively [4].

[1] E. Majorana, Nuovo Cimento **14**, 171 (1937).
[2] J. C. Pati and A. Salam, Phys. Rev. D **10**, 275 (1974); **11**, 703(E) (1975); R. N. Mohapatra and G. Senjanovic, Phys. Rev. Lett. **44**, 912 (1980).
[3] D. Rajaram *et al.*, Phys. Rev. Lett. **94**, 181801 (2005).
[4] K. W. Edwards *et al.*, Phys. Rev. D **65**, 111102 (2002).
[5] J. J. Gomez-Cadenas, J. Martin-Albo, M. Mezzetto, F. Monrabal, and M. Sorel, Riv. Nuovo Cimento **35**, 29 (2012).
[6] G. Aad *et al.*, J. High Energy Phys. 10 (2011) 107.
[7] S. Pascoli and S. T. Petcov, Phys. Rev. D **77**, 113003 (2008).
[8] A. Atre, T. Han, S. Pascoli, and B. Zhang, J. High Energy Phys. 05 (2009) 030.
[9] V. Rentala, W. Shepherd, and S. Su, Phys. Rev. D **84**, 035004 (2011).
[10] C. Picciotto, Phys. Rev. D **56**, 1612 (1997).
[11] A. Augusto Alves *et al.*, JINST **3**, S08005 (2008).
[12] T. Sjöstrand, S. Mrenna, and P. Z. Skands, J. High Energy Phys. 05 (2006) 026.
[13] S. Agostinelli *et al.*, Nucl. Instrum. Methods Phys. Res., Sect. A **506** 250 (2003).
[14] R Aaij *et al.*, Phys. Lett. B **699**, 330 (2011).
[15] T. Skwarnicki, Ph.D. thesis, Institute of Nuclear Physics, Krakow, 1986 [Report No. DESY-F31-86-02].
[16] K. Nakamura *et al.*, J. Phys. G **37**, 075021 (2010).

R. Aaij,[23] C. Abellan Beteta,[35,a] B. Adeva,[36] M. Adinolfi,[42] C. Adrover,[6] A. Affolder,[48] Z. Ajaltouni,[5] J. Albrecht,[37] F. Alessio,[37] M. Alexander,[47] G. Alkhazov,[29] P. Alvarez Cartelle,[36] A. A. Alves, Jr.,[22] S. Amato,[2] Y. Amhis,[38] J. Anderson,[39] R. B. Appleby,[50] O. Aquines Gutierrez,[10] F. Archilli,[18,37] L. Arrabito,[53] A. Artamonov,[34] M. Artuso,[52,37] E. Aslanides,[6] G. Auriemma,[22,b] S. Bachmann,[11] J. J. Back,[44] D. S. Bailey,[50] V. Balagura,[30,37] W. Baldini,[16] R. J. Barlow,[50] C. Barschel,[37] S. Barsuk,[7] W. Barter,[43] A. Bates,[47] C. Bauer,[10] Th. Bauer,[23] A. Bay,[38] I. Bediaga,[1] K. Belous,[34] I. Belyaev,[30,37] E. Ben-Haim,[8] M. Benayoun,[8] G. Bencivenni,[18] S. Benson,[46] J. Benton,[42] R. Bernet,[39] M.-O. Bettler,[17] M. van Beuzekom,[23] A. Bien,[11] S. Bifani,[12] A. Bizzeti,[17,c] P. M. Bjørnstad,[50] T. Blake,[49] F. Blanc,[38] C. Blanks,[49] J. Blouw,[11] S. Blusk,[52] A. Bobrov,[33] V. Bocci,[22] A. Bondar,[33] N. Bondar,[29] W. Bonivento,[15] S. Borghi,[47] A. Borgia,[52] T. J. V. Bowcock,[48] C. Bozzi,[16] T. Brambach,[9] J. van den Brand,[24] J. Bressieux,[38] D. Brett,[50] S. Brisbane,[51] M. Britsch,[10] T. Britton,[52] N. H. Brook,[42] H. Brown,[48] A. Büchler-Germann,[39] I. Burducea,[28] A. Bursche,[39] J. Buytaert,[37] S. Cadeddu,[15] J. M. Caicedo Carvajal,[37] O. Callot,[7] M. Calvi,[20,d] M. Calvo Gomez,[35,a] A. Camboni,[35] P. Campana,[18,37] A. Carbone,[14] G. Carboni,[21,e] R. Cardinale,[19,37,f] A. Cardini,[15] L. Carson,[36] K. Carvalho Akiba,[23] G. Casse,[48] M. Cattaneo,[37] M. Charles,[51] Ph. Charpentier,[37] N. Chiapolini,[39] K. Ciba,[37] X. Cid Vidal,[36] G. Ciezarek,[49] P. E. L. Clarke,[46,37] H. V. Cliff,[43] J. Closier,[37] C. Coca,[28] V. Coco,[23] J. Cogan,[6] P. Collins,[37] A. Comerma-Montells,[35] F. Constantin,[28] G. Conti,[38] A. Contu,[51] A. Cook,[42] M. Coombes,[42] G. Corti,[37] G. A. Cowan,[38] R. Currie,[46] B. D'Almagne,[7] C. D'Ambrosio,[37] P. David,[8] I. De Bonis,[4] S. De Capua,[21,e] M. De Cian,[39] F. De Lorenzi,[12] J. M. De Miranda,[1] L. De Paula,[2] P. De Simone,[18] D. Decamp,[4] M. Deckenhoff,[9] H. Degaudenzi,[38,37] M. Deissenroth,[11] L. Del Buono,[8] C. Deplano,[15] O. Deschamps,[5] F. Dettori,[15,g] J. Dickens,[43] H. Dijkstra,[37] P. Diniz Batista,[1] F. Domingo Bonal,[35,a] S. Donleavy,[48] A. Dosil Suárez,[36] D. Dossett,[44] A. Dovbnya,[40] F. Dupertuis,[38] R. Dzhelyadin,[34] S. Easo,[45] U. Egede,[49] V. Egorychev,[30] S. Eidelman,[33] D. van Eijk,[23] F. Eisele,[11] S. Eisenhardt,[46] R. Ekelhof,[9] L. Eklund,[47] Ch. Elsasser,[39] D. G. d'Enterria,[35,h] D. Esperante Pereira,[36] L. Estève,[43] A. Falabella,[16,i] E. Fanchini,[20,d] C. Färber,[11] G. Fardell,[46] C. Farinelli,[23] S. Farry,[12] V. Fave,[38] V. Fernandez Albor,[36] M. Ferro-Luzzi,[37] S. Filippov,[32] C. Fitzpatrick,[46] M. Fontana,[10] F. Fontanelli,[19,f] R. Forty,[37] M. Frank,[37] C. Frei,[37] M. Frosini,[17,37,j] S. Furcas,[20] A. Gallas Torreira,[36] D. Galli,[14,k] M. Gandelman,[2] P. Gandini,[51] Y. Gao,[3] J-C. Garnier,[37] J. Garofoli,[52] J. Garra Tico,[43] L. Garrido,[35] D. Gascon,[35] C. Gaspar,[37] N. Gauvin,[38] M. Gersabeck,[37] T. Gershon,[44,37] Ph. Ghez,[4] V. Gibson,[43] V. V. Gligorov,[37] C. Göbel,[54] D. Golubkov,[30] A. Golutvin,[49,30,37] A. Gomes,[2] H. Gordon,[51] M. Grabalosa Gándara,[35] R. Graciani Diaz,[35] L. A. Granado Cardoso,[37] E. Graugés,[35] G. Graziani,[17] A. Grecu,[28] E. Greening,[51] S. Gregson,[43] B. Gui,[52] E. Gushchin,[32] Yu. Guz,[34] T. Gys,[37] G. Haefeli,[38] C. Haen,[37] S. C. Haines,[43]

T. Hampson,[42] S. Hansmann-Menzemer,[11] R. Harji,[49] N. Harnew,[51] J. Harrison,[50] P. F. Harrison,[44] J. He,[7]
V. Heijne,[23] K. Hennessy,[48] P. Henrard,[5] J. A. Hernando Morata,[36] E. van Herwijnen,[37] E. Hicks,[48] W. Hofmann,[10]
K. Holubyev,[11] P. Hopchev,[4] W. Hulsbergen,[23] P. Hunt,[51] T. Huse,[48] R. S. Huston,[12] D. Hutchcroft,[48] D. Hynds,[47]
V. Iakovenko,[41] P. Ilten,[12] J. Imong,[42] R. Jacobsson,[37] A. Jaeger,[11] M. Jahjah Hussein,[5] E. Jans,[23] F. Jansen,[23]
P. Jaton,[38] B. Jean-Marie,[7] F. Jing,[3] M. John,[51] D. Johnson,[51] C. R. Jones,[43] B. Jost,[37] S. Kandybei,[40] M. Karacson,[37]
T. M. Karbach,[9] J. Keaveney,[12] U. Kerzel,[37] T. Ketel,[24] A. Keune,[38] B. Khanji,[6] Y. M. Kim,[46] M. Knecht,[38]
S. Koblitz,[37] P. Koppenburg,[23] A. Kozlinskiy,[23] L. Kravchuk,[32] K. Kreplin,[11] M. Kreps,[44] G. Krocker,[11]
P. Krokovny,[11] F. Kruse,[9] K. Kruzelecki,[37] M. Kucharczyk,[20,25,37] S. Kukulak,[25] R. Kumar,[14,37]
T. Kvaratskheliya,[30,37] V. N. La Thi,[38] D. Lacarrere,[37] G. Lafferty,[50] A. Lai,[15] D. Lambert,[46] R. W. Lambert,[37]
E. Lanciotti,[37] G. Lanfranchi,[18] C. Langenbruch,[11] T. Latham,[44] R. Le Gac,[6] J. van Leerdam,[23] J.-P. Lees,[4]
R. Lefèvre,[5] A. Leflat,[31,37] J. Lefrançois,[7] O. Leroy,[6] T. Lesiak,[25] L. Li,[3] L. Li Gioi,[5] M. Lieng,[9] M. Liles,[48]
R. Lindner,[37] C. Linn,[11] B. Liu,[3] G. Liu,[37] J. H. Lopes,[2] E. Lopez Asamar,[35] N. Lopez-March,[38] J. Luisier,[38]
F. Machefert,[7] I. V. Machikhiliyan,[4,30] F. Maciuc,[10] O. Maev,[29,37] J. Magnin,[1] S. Malde,[51] R. M. D. Mamunur,[37]
G. Manca,[15,g] G. Mancinelli,[6] N. Mangiafave,[43] U. Marconi,[14] R. Märki,[38] J. Marks,[11] G. Martellotti,[22] A. Martens,[7]
L. Martin,[51] A. Martín Sánchez,[7] D. Martinez Santos,[37] A. Massafferri,[1] Z. Mathe,[12] C. Matteuzzi,[20] M. Matveev,[29]
E. Maurice,[6] B. Maynard,[52] A. Mazurov,[16,32,37] G. McGregor,[50] R. McNulty,[12] C. Mclean,[14] M. Meissner,[11]
M. Merk,[23] J. Merkel,[9] R. Messi,[21,e] S. Miglioranzi,[37] D. A. Milanes,[13,37] M.-N. Minard,[4] S. Monteil,[5] D. Moran,[12]
P. Morawski,[25] R. Mountain,[52] I. Mous,[23] F. Muheim,[46] K. Müller,[39] R. Muresan,[28,38] B. Muryn,[26] M. Musy,[35]
J. Mylroie-Smith,[48] P. Naik,[42] T. Nakada,[38] R. Nandakumar,[45] J. Nardulli,[45] I. Nasteva,[1] M. Nedos,[9] M. Needham,[46]
N. Neufeld,[37] C. Nguyen-Mau,[38,l] M. Nicol,[7] S. Nies,[9] V. Niess,[5] N. Nikitin,[31] A. Nomerotski,[51]
A. Oblakowska-Mucha,[26] V. Obraztsov,[34] S. Oggero,[23] S. Ogilvy,[47] O. Okhrimenko,[41] R. Oldeman,[15,g]
M. Orlandea,[28] J. M. Otalora Goicochea,[2] P. Owen,[49] K. Pal,[52] J. Palacios,[39] A. Palano,[13,g] M. Palutan,[18]
J. Panman,[37] A. Papanestis,[45] M. Pappagallo,[13,m] C. Parkes,[47,37] C. J. Parkinson,[49] G. Passaleva,[17] G. D. Patel,[48]
M. Patel,[49] S. K. Paterson,[49] G. N. Patrick,[45] C. Patrignani,[19,f] C. Pavel-Nicorescu,[28] A. Pazos Alvarez,[36]
A. Pellegrino,[23] G. Penso,[22,n] M. Pepe Altarelli,[37] S. Perazzini,[14,k] D. L. Perego,[20,d] E. Perez Trigo,[36]
A. Pérez-Calero Yzquierdo,[35] P. Perret,[5] M. Perrin-Terrin,[6] G. Pessina,[20] A. Petrella,[16,37] A. Petrolini,[19,f]
E. Picatoste Olloqui,[35] B. Pie Valls,[35] B. Pietrzyk,[4] T. Pilar,[44] D. Pinci,[22] R. Plackett,[47] S. Playfer,[46]
M. Plo Casasus,[36] G. Polok,[25] A. Poluektov,[44,33] E. Polycarpo,[2] D. Popov,[10] B. Popovici,[28] C. Potterat,[35] A. Powell,[51]
T. du Pree,[23] J. Prisciandaro,[38] V. Pugatch,[41] A. Puig Navarro,[35] W. Qian,[52] J. H. Rademacker,[42]
B. Rakotomiaramanana,[38] M. S. Rangel,[2] I. Raniuk,[40] G. Raven,[24] S. Redford,[51] M. M. Reid,[44] A. C. dos Reis,[1]
S. Ricciardi,[45] K. Rinnert,[48] D. A. Roa Romero,[5] P. Robbe,[7] E. Rodrigues,[47] F. Rodrigues,[2] P. Rodriguez Perez,[36]
G. J. Rogers,[43] S. Roiser,[37] V. Romanovsky,[34] M. Rosello,[35,a] J. Rouvinet,[38] T. Ruf,[37] H. Ruiz,[35] G. Sabatino,[21,e]
J. J. Saborido Silva,[36] N. Sagidova,[29] P. Sail,[47] B. Saitta,[15,g] C. Salzmann,[39] M. Sannino,[19,f] R. Santacesaria,[22]
R. Santinelli,[37] E. Santovetti,[21,e] M. Sapunov,[6] A. Sarti,[18,n] C. Satriano,[22,b] A. Satta,[21] M. Savrie,[16,i] D. Savrina,[30]
P. Schaack,[49] M. Schiller,[11] S. Schleich,[9] M. Schmelling,[10] B. Schmidt,[37] O. Schneider,[38] A. Schopper,[37]
M.-H. Schune,[7] R. Schwemmer,[37] B. Sciascia,[18] A. Sciubba,[18,n] M. Seco,[36] A. Semennikov,[30] K. Senderowska,[26]
I. Sepp,[49] N. Serra,[39] J. Serrano,[6] P. Seyfert,[11] B. Shao,[3] M. Shapkin,[34] I. Shapoval,[40,37] P. Shatalov,[30] Y. Shcheglov,[29]
T. Shears,[48] L. Shekhtman,[33] O. Shevchenko,[40] V. Shevchenko,[30] A. Shires,[49] R. Silva Coutinho,[54] H. P. Skottowe,[43]
T. Skwarnicki,[52] A. C. Smith,[37] N. A. Smith,[48] E. Smith,[51,45] K. Sobczak,[5] F. J. P. Soler,[47] A. Solomin,[42] F. Soomro,[49]
B. Souza De Paula,[2] B. Spaan,[9] A. Sparkes,[46] P. Spradlin,[47] F. Stagni,[37] S. Stahl,[11] O. Steinkamp,[39] S. Stoica,[28]
S. Stone,[52,37] B. Storaci,[23] M. Straticiuc,[28] U. Straumann,[39] N. Styles,[46] V. K. Subbiah,[37] S. Swientek,[9]
M. Szczekowski,[27] P. Szczypka,[38] T. Szumlak,[26] S. T'Jampens,[4] E. Teodorescu,[28] F. Teubert,[37] C. Thomas,[51,45]
E. Thomas,[37] J. van Tilburg,[11] V. Tisserand,[4] M. Tobin,[39] S. Topp-Joergensen,[51] N. Torr,[51] M. T. Tran,[38]
A. Tsaregorodtsev,[6] N. Tuning,[23] A. Ukleja,[27] P. Urquijo,[52] U. Uwer,[11] V. Vagnoni,[14] G. Valenti,[14]
R. Vazquez Gomez,[35] P. Vazquez Regueiro,[36] S. Vecchi,[16] J. J. Velthuis,[42] M. Veltri,[17,o] K. Vervink,[37] B. Viaud,[7]
I. Videau,[7] X. Vilasis-Cardona,[35,a] J. Visniakov,[36] A. Vollhardt,[39] D. Voong,[42] A. Vorobyev,[29] H. Voss,[10] K. Wacker,[9]
S. Wandernoth,[11] J. Wang,[52] D. R. Ward,[43] A. D. Webber,[50] D. Websdale,[49] M. Whitehead,[44] D. Wiedner,[11]
L. Wiggers,[23] G. Wilkinson,[51] M. P. Williams,[44,45] M. Williams,[49] F. F. Wilson,[45] J. Wishahi,[9] M. Witek,[25]
W. Witzeling,[37] S. A. Wotton,[43] K. Wyllie,[37] Y. Xie,[46] F. Xing,[51] Z. Xing,[52] Z. Yang,[3] R. Young,[46] O. Yushchenko,[34]
M. Zavertyaev,[10,p] L. Zhang,[52] W. C. Zhang,[12] Y. Zhang,[3] A. Zhelezov,[11] L. Zhong,[3] E. Zverev,[31] and A. Zvyagin[37]

(LHCb Collaboration)

[1]Centro Brasileiro de Pesquisas Físicas (CBPF), Rio de Janeiro, Brazil
[2]Universidade Federal do Rio de Janeiro (UFRJ), Rio de Janeiro, Brazil
[3]Center for High Energy Physics, Tsinghua University, Beijing, China
[4]LAPP, Université de Savoie, CNRS/IN2P3, Annecy-Le-Vieux, France
[5]Clermont Université, Université Blaise Pascal, CNRS/IN2P3, LPC, Clermont-Ferrand, France
[6]CPPM, Aix-Marseille Université, CNRS/IN2P3, Marseille, France
[7]LAL, Université Paris-Sud, CNRS/IN2P3, Orsay, France
[8]LPNHE, Université Pierre et Marie Curie, Université Paris Diderot, CNRS/IN2P3, Paris, France
[9]Fakultät Physik, Technische Universität Dortmund, Dortmund, Germany
[10]Max-Planck-Institut für Kernphysik (MPIK), Heidelberg, Germany
[11]Physikalisches Institut, Ruprecht-Karls-Universität Heidelberg, Heidelberg, Germany
[12]School of Physics, University College Dublin, Dublin, Ireland
[13]Sezione INFN di Bari, Bari, Italy
[14]Sezione INFN di Bologna, Bologna, Italy
[15]Sezione INFN di Cagliari, Cagliari, Italy
[16]Sezione INFN di Ferrara, Ferrara, Italy
[17]Sezione INFN di Firenze, Firenze, Italy
[18]Laboratori Nazionali dell'INFN di Frascati, Frascati, Italy
[19]Sezione INFN di Genova, Genova, Italy
[20]Sezione INFN di Milano Bicocca, Milano, Italy
[21]Sezione INFN di Roma Tor Vergata, Roma, Italy
[22]Sezione INFN di Roma La Sapienza, Roma, Italy
[23]Nikhef National Institute for Subatomic Physics, Amsterdam, The Netherlands
[24]Nikhef National Institute for Subatomic Physics and Vrije Universiteit, Amsterdam, The Netherlands
[25]Henryk Niewodniczanski Institute of Nuclear Physics Polish Academy of Sciences, Cracow, Poland
[26]Faculty of Physics & Applied Computer Science, Cracow, Poland
[27]Soltan Institute for Nuclear Studies, Warsaw, Poland
[28]Horia Hulubei National Institute of Physics and Nuclear Engineering, Bucharest-Magurele, Romania
[29]Petersburg Nuclear Physics Institute (PNPI), Gatchina, Russia
[30]Institute of Theoretical and Experimental Physics (ITEP), Moscow, Russia
[31]Institute of Nuclear Physics, Moscow State University (SINP MSU), Moscow, Russia
[32]Institute for Nuclear Research of the Russian Academy of Sciences (INR RAN), Moscow, Russia
[33]Budker Institute of Nuclear Physics (SB RAS) and Novosibirsk State University, Novosibirsk, Russia
[34]Institute for High Energy Physics (IHEP), Protvino, Russia
[35]Universitat de Barcelona, Barcelona, Spain
[36]Universidad de Santiago de Compostela, Santiago de Compostela, Spain
[37]European Organization for Nuclear Research (CERN), Geneva, Switzerland
[38]Ecole Polytechnique Fédérale de Lausanne (EPFL), Lausanne, Switzerland
[39]Physik-Institut, Universität Zürich, Zürich, Switzerland
[40]NSC Kharkiv Institute of Physics and Technology (NSC KIPT), Kharkiv, Ukraine
[41]Institute for Nuclear Research of the National Academy of Sciences (KINR), Kyiv, Ukraine
[42]H. H. Wills Physics Laboratory, University of Bristol, Bristol, United Kingdom
[43]Cavendish Laboratory, University of Cambridge, Cambridge, United Kingdom
[44]Department of Physics, University of Warwick, Coventry, United Kingdom
[45]STFC Rutherford Appleton Laboratory, Didcot, United Kingdom
[46]School of Physics and Astronomy, University of Edinburgh, Edinburgh, United Kingdom
[47]School of Physics and Astronomy, University of Glasgow, Glasgow, United Kingdom
[48]Oliver Lodge Laboratory, University of Liverpool, Liverpool, United Kingdom
[49]Imperial College London, London, United Kingdom
[50]School of Physics and Astronomy, University of Manchester, Manchester, United Kingdom
[51]Department of Physics, University of Oxford, Oxford, United Kingdom
[52]Syracuse University, Syracuse, New York, USA
[53]CC-IN2P3, CNRS/IN2P3, Lyon-Villeurbanne, France
[54]Pontifícia Universidade Católica do Rio de Janeiro (PUC-Rio), Rio de Janeiro, Brazil;
Universidade Federal do Rio de Janeiro (UFRJ), Rio de Janeiro, Brazil

[a]Also at LIFAELS, La Salle, Universitat Ramon Llull, Barcelona, Spain.

[b]Also at Università della Basilicata, Potenza, Italy.

[c]Also at Università di Modena e Reggio Emilia, Modena, Italy.

[d]Also at Università di Milano Bicocca, Milano, Italy.

[e]Also at Università di Roma Tor Vergata, Roma, Italy.

[f]Also at Università di Genova, Genova, Italy.

[g]Also at Università di Cagliari, Cagliari, Italy.

[h]Also at Institució Catalana de Recerca i Estudis Avançats (ICREA), Barcelona, Spain.

[i]Also at Università di Ferrara, Ferrara, Italy.

[j]Also at Università di Firenze, Firenze, Italy.

[k]Also at Università di Bologna, Bologna, Italy.

[l]Also at Hanoi University of Science, Hanoi, Vietnam.

[m]Also at Università di Bari, Bari, Italy

[n]Also at Università di Roma La Sapienza, Roma, Italy.

[o]Also at Università di Urbino, Urbino, Italy.

[p]Also at P.N. Lebedev Physical Institute, Russian Academy of Science (LPI RAS), Moscow, Russia.